Design and Measurements of a C-Band Array for High Power High Bandwidth SAR Application

Alberto Di Maria, Markus Limbach, Ralf Horn, Andreas Reigber
Microwaves and Radar Institute
German Aerospace Center (DLR)
Oberpfaffenhofen, Germany
Alberto.DiMaria@dlr.de

***Abstract*— The design and test of a dual linear polarized C-Band antenna for the airborne Synthetic Aperture Radar (SAR) system of DLR is presented. Distinctive features are dual polarization, high bandwidth, high power handling and a modular construction.**

Index Terms*— *C-Band; Synthetic Aperture Radar; dual linear polarization; high power; modular design

I. INTRODUCTION

The Microwaves and Radar Institute at the German Aerospace Center in Oberpfaffenhofen operates an airborne imaging radar named F-SAR [1]. It is a highly flexible Synthetic Aperture Radar (SAR) that is able to operate in a wide range of wavelengths starting from 1 meter down to 3 centimeters. This radar system makes it possible to test several polarimetric and interferometric techniques as well as corresponding processing algorithms. It is also an excellent test bed for investigating the expected system performance when designing SAR satellites.

In C-Band (5.3GHz) this radar is able to operate in dual linear polarization with 2.2kW pulse power (5% duty cycle) and 800MHz bandwidth. As the footprint of the radiated beam directly affects the SAR performance, the beamwidth, the side lobe level (SLL) and the overall stability of the beam shape over the frequency band are other key specifications for the antenna. Finally, good cross-polarization isolation is desirable.

This paper details the design of the antenna that operates in this frequency range, from the initial concept to the prototype realization. Then, results of actual measurements are presented and, finally, an image acquired by the radar through this antenna is shown.

II. ANTENNA DESIGN

A. Modular design

The antenna is a planar array consisting of 18 patches organized in a 6×3 configuration. The 3 rows are designed and realized as separated modules, so that the array can be reorganized without requiring a complete re-design (e.g. a larger 4x6 array can be easily realized by adding a row module). The feeding network is consequently divided in two separate levels, as schematically described in Fig.1. Each module implements the lower level, which feeds the radiating patches in both polarizations and enables beam shaping in the azimuth direction. The modules are in turn fed by two higher level feeding networks (one per polarization), which provide the beam shaping and a certain degree of beam steering in the elevation direction. This separation allows focusing on the critical aspects of the two feeding networks. The first level is specifically designed to withstand the high output power of the radar. In the second level the power is not a critical issue anymore and the design is focused on the sensitivity and the cross-polarization isolation.

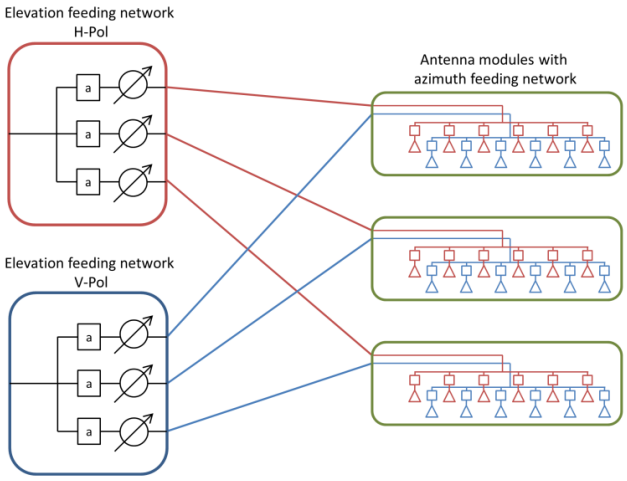

Figure 1. Modular structure of the antenna. The first level of the feeding network (elevation) provides the tapering and the beam steering in elevation direction. The second level provides the tapering in azimuth direction.

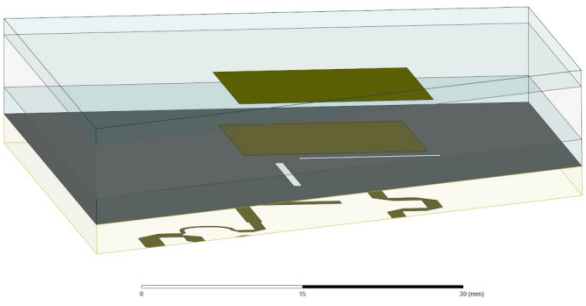

Figure 2. Layers structure of the radiating module. The two stacked patches are coupled to the feeding microstrip lines by means of a slot in the ground plane.

B. *Array module*

The radiating element consists of two stacked microstrip patches that are coupled to a microstrip line by a slot in the intervening ground plane [2], [3]. Fig. 2 shows the structure of the module layers. The patches substrate material is the RT/Duroid™ 5880, with a low dielectric constant ($\epsilon_r = 2.2$). The outer patch is mounted upside down, so that the substrate itself acts as a radome for the antenna. For this reason has been used a dielectric which has an excellent chemical resistance and a low moisture absorption.

The feeding network supplies a tapered voltage feed in order to obtain an SLL=-20dB. In place of traditional T-junction power dividers, commonly used in networks realized in microstrip technology, this azimuth feeding network employs split-tee power dividers [4]. This solution provides for superior receiving performance at the expense of a more complicated realization as a lumped resistor has to be inserted in a multilayer design. The substrate material for the feeding network is the Rogers TMM™ 4 ($\epsilon_r = 4.5$).

Finally, techniques aiming to obtain high cross-polarization suppression are used [5]. The elements in the array have not the same orientation; they are instead organized in pairs of mirrored patches as can be observed in Fig. 3. When vertical polarization is desired, the V-ports must be excited in phase. When horizontal polarization is desired the two H-ports in each pair must be excited 180° out of phase to obtain the same effective excitations of the elements equally oriented. This configuration leads to a cross-polarization isolation greater than 30dB (Fig. 8).

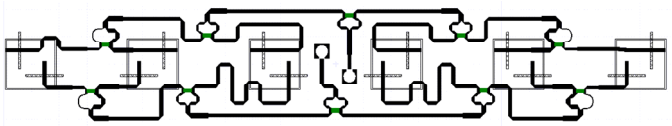

Figure 3. Array module feeding network. It provides the beam shaping in azimuth direction. Each patch couple is fed by two slots. The technique of mirroring pairs of elements can be noted.

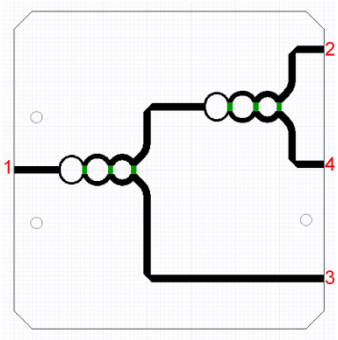

Figure 4. Elevation feeding network. Two cascaded three-stage Wilkinson power dividers are employed.

C. *Elevation feeding network module*

The upper level feeding network has to withstand the radar output power, equal to 2.2kW peak-to-peak. The chosen substrate material is the RT/Duroid™ 6035HTC, that is characterized by high thermal conductivity for improved dielectric heat dissipation. The resistors are high power SMD components and special care has been taken to solder these components to a via-patch on the board's top surface to transfer the generated heat to the ground plane.

When dealing with such power, reflection on the input port of the antenna can easily damage the radar receiving section. This reflection needs to be minimized and consequently a matching better than -15dB over the entire bandwidth is required. The deigned network is a 3-way power divider realized with two cascaded multistage Wilkinson power splitters as shown in Fig. 4. The multistage architecture provides enough degrees of freedom to optimize both matching and bandwidth.

III. ANTENNA SIMULATION

The antenna was designed using Ansys HFSS and Ansys Designer software. Each antenna component was simulated separately and tuned to meet dimensional and frequency requirements with a fully parameterized model. These components include transmission lines, split-tee power dividers, the stacked patch antenna element itself, the multistage Wilkinson dividers, the resistors and even the connectors. The individual components are then assembled and interconnected in the circuit simulator to form the whole array and the elevation feeding network. The assembly obtained is then further optimized to match all the antenna requirements, with the advantage of a fully parameterized model and the speed of a circuit simulator, but maintaining, at the same time, the accuracy of a full wave analysis of the entire model. Fig. 5 shows the simulated radiation pattern in azimuth direction for both polarizations.

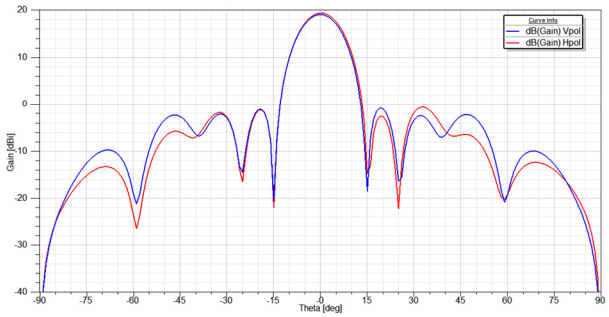

Figure 5. Simulated radiation pattern in the azimuth cut. The red line is the horizontal polarization, whereas the blue one is the vertical polarization.

IV. ANTENNA MEASUREMENTS

A prototype of this antenna, shown in Fig. 6, was completely assembled in the Microwaves and Radar Institute in DLR and its performance was measured in the Compact Test Range Facility of the above mentioned Institute [6].

Fig. 7 shows the measured radiation pattern in the two principal cut planes. The upper graph shows the pattern in the azimuth direction; the gain is 18dBi, the side lobe level is -18dB and the beamwidth is 12deg. The plot is in good agreement with the simulation results. The lower graph shows the pattern in the elevation direction; the beam is electrically steered by 7deg down looking (the horizon is located at 0deg) and the beamwidth is 24deg. Fig. 8 shows the cross-polar component of the radiated field for both polarization, the color code is the same as Fig. 7 and the values are normalized with respect to the maximum antenna gain. As can be observed the chosen patch orientation, described in the paragraph II.B, improves significantly the cross-polarization isolation.

Fig. 9 shows a particular plot aiming to illustrate the stability of the beam shape over the frequency bandwidth. The graph is a contour plot of the radiation pattern in azimuth direction over the frequency. To understand this plot, we can imagine building a three-dimensional plot spanning the pattern of Fig. 7 over the frequency. Fig. 9 is like the top view of this hypothetical 3D plot. The parallelity of the contour lines is an indication of the stability of the beam shape over the frequency.

The elevation feeding network was also tested separately. The transmission and the matching of the ports were measured by means of a 4-ports network analyzer. Fig. 10 shows the measured S_{21}, S_{31} and S_{41} from 4.3GHz to 6.3GHz. The transmission is practically constant over the entire bandwidth and the insertion loss can be evaluated to 0.4dB. Fig. 11 shows the measured matching at the input port of the power divider: the multistage architecture has proven its effectiveness also in this excellent result.

As said, the elevation feeding network has to withstand to the high output power of the radar. The maximum peak power is equal to 2.2kW and, considering a 5% duty cycle, the maximum mean power is equal to 110W. In order to test the resistance of the components to such stress, a high power measurement using the actual radar as source was done. Fig. 12 shows an infrared picture of the network during these measurements. Even though the SMD resistors have reached the maximum temperature of 80°C, the special substrate was able to conduct away the generated heat very quickly and no failure was registered under any test cycle.

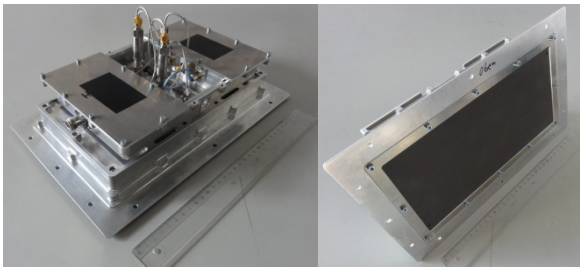

Figure 6. Picture of the assembled prototype.

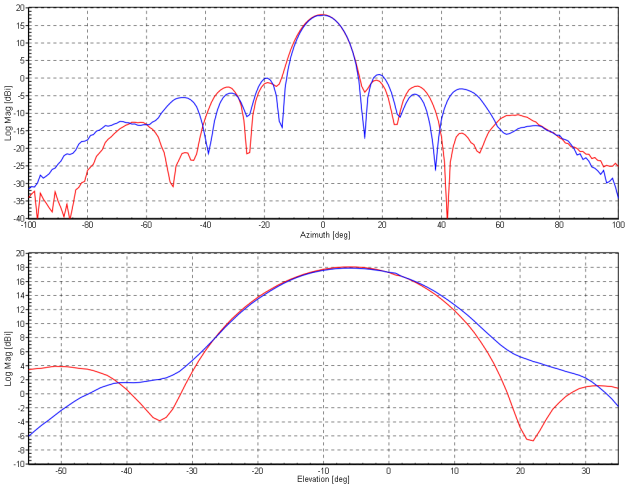

Figure 7. Measured radiation pattern in the two principal cut planes. The upper graph shows the azimuth cut and the lower one the elevation cut. The red line is the horizontal polarization, whereas the blue one is the vertical polarization.

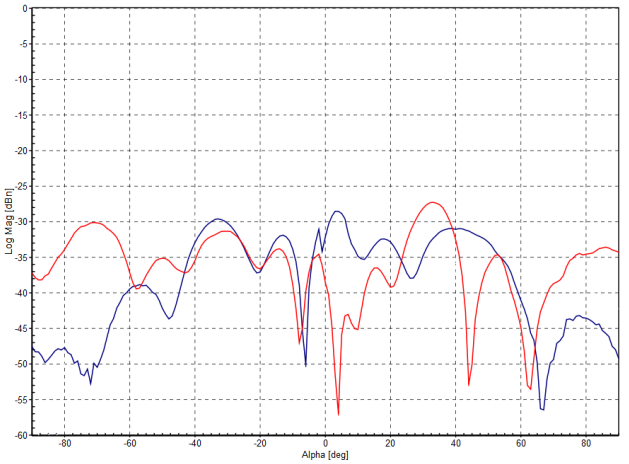

Figure 8. Measured cross-polar component of the radiated field. The color code is the same as Fig. 7. The values are normalized with respect to the maximum antenna gain to highlight the cross-polarization isolation.

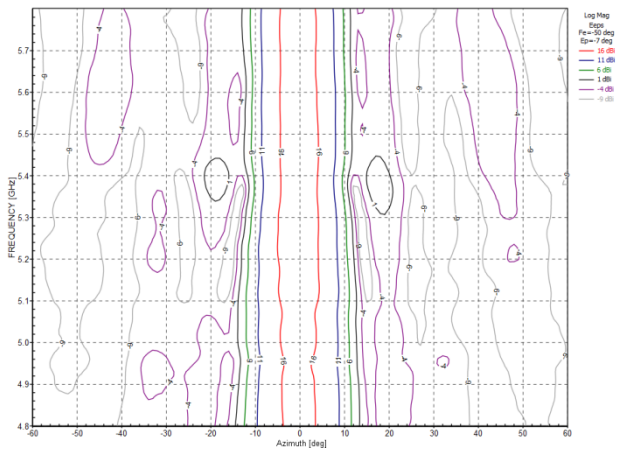

Figure 9. Contour plot of the radiation pattern in azimuth direction over the frequency. Please, refer to the text for a description of this plot. The parallelity of the contour lines is an indication of the stability of the beam shape over the frequency.

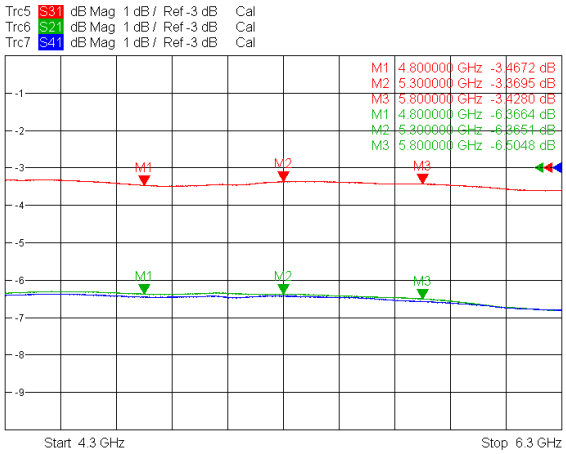

Figure 10. Elevation feeding network measurements. The transmission to the three output ports is shown over 2GHz bandwidth. The port numbering corresponds to the labels indicated in Fig. 4.

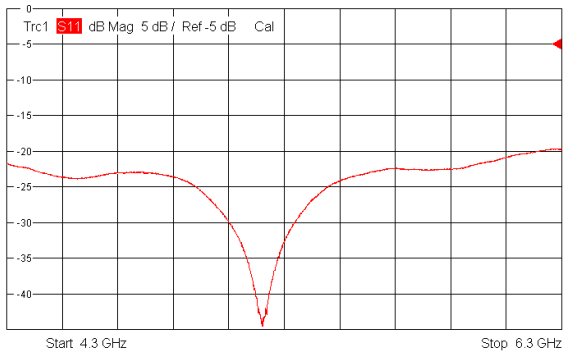

Figure 11. Elevation feeding network measurements. The matching at the input port is shown over 2GHz bandwidth. The port numbering corresponds to the labels indicated in Fig. 4.

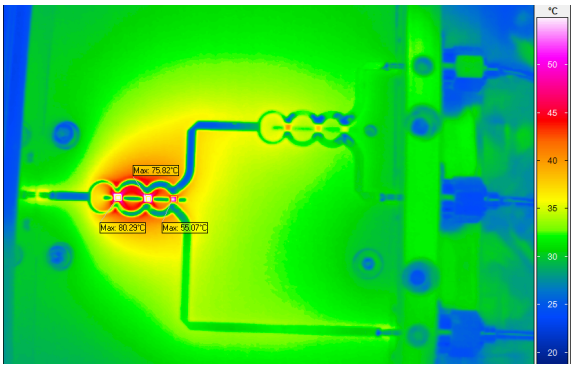

Figure 12. Infrared picture of the elevation feeding network, taken during the high power measurements. The SMD resistors have reached the maximum temperature of 80°C, but the substrate is able to conduct away the generated heat very quickly.

V. FINAL REMARKS

The antenna was finally built in two exemplars, installed on the airplane and used in two F-SAR campaigns up to now [1]. Fig. 13 shows a C-Band acquisition of the Kaufbeuren military base taken during the first flight. With respect to the picture, the airplane flew from left to right and the top of the image is near range, whereas the bottom is far range. A specular reflection with a strong signal coming back to the radar (like the buildings and to a lesser extent the trees) produces a bright color in the image. On the other hand a flat surface reflects the signal away from the radar and produces a dark color: the landing strip is an example. Under the buildings and the trees can be observed what seems to be a shadow. This is indeed like a shadow: the dark color is due to the absence of signal that has been shielded by the target itself. The shadow orientation also reveals that the signal source (i.e. the airplane) is located on the top of the image.

Figure 13. C-Band SAR acquisition of the Kaufbeuren military base obtained using the described antenna.

REFERENCES

[1] R. Horn, A. Nottensteiner, A. Reigber, J. Fischer and R. Scheiber, "SAR- DLR's new multifrequency polarimetric airborne SAR", IGARSS, 2009.

[2] D. M. Pozar, "A microstrip antenna aperture coupled to a microstrip line", Electron. Lett., vol. 21, no. 2, Jan. 1985, pp. 49-50.

[3] F. Croq and A. Papiernik, "Stacked Slot-Coupled Printed Antenna", IEEE Microwave and Guided Wave Letters, vol. 1, no. 10, Oct. 1991, pp. 288-290.

[4] L. I. Parad and R. L. Moynihan, "Split-Tee Power Divider", IEEE Trnsaction on Microwave Theory and Techniques, Jan. 1965, pp. 91-95.

[5] K. Woelders and J. Granholm, "Cross-Polarization and Sidelobe Suppression in Dual Linear Polarization Antenna Arrays", IEEE Transactions on Antennas and Propagation, vol. 45, no. 12, Dec. 1997, pp. 1727-1740.

[6] M. Limbach, B. Gabler, R. Horn, A. Reigber, "DLR-HR Compact Test Range Facility", European Conference on Antennas and Propagation EUCAP 2009, Berlin, 23-27 March 2009.